

STRUCTURAL PROPERTIES OF HELICOPTER ROTOR BLADE SECTIONS

Graham F.J. Hill and Paul M. Weaver

Department of Aerospace Engineering, Queen's Building, University of Bristol, Bristol,
England, UK, BS8 1TR

Abstract

A finite element based method for calculating the structural properties of helicopter rotor blades is presented. In contrast to other formulations, a full 6x6 stiffness matrix is produced with all coupling behaviour represented. It is capable of dealing with anisotropic, orthotropic and isotropic material properties within the section. Both static and dynamic behaviour results for beams and rotor blades with various sections are presented.

Introduction

From a modelling perspective, one of the most complicated closed section beam-type structures of practical importance is a helicopter rotor blade. They are both complex in construction and structural response. Typically they may be 6-10m in length with chord lengths and depths approximately 650mm wide and 100mm deep, respectively. Furthermore, since the 1970s they have been constructed from highly anisotropic composite materials (Carbon fibre/epoxy, Rohacell foam and Nomex honeycomb). Structurally, they may be considered as slender one-dimensional elements subject to extensional (centrifugal), twisting and bi-directional (flap and lag) bending loads. Their behavioural response is further complicated by intrinsic coupling between

- centrifugal loads and twisting
- torsional loads and extension
- flexural loads and twisting
- torsional moment and flexure

due to the non-coincidence of shear, flexural and mass centres that stems from the asymmetric nature of the cross-section and material response. Indeed the latter type of coupling has been the centre of much attention since Mansfield and Sobey [1] raised the possibility of aeroelastic coupling on tailoring dynamic performance.

The analysis of complex structures such as a helicopter rotor blade, at present, is practically impossible due to the amount of memory required. The amount of data for any 3-dimensional finite element model with sufficient elements to provide detailed stress-strain response is prohibitively large, and generally impossible to solve on anything other than the largest supercomputers.

Herein, lies the crux of the problem, to apply appropriate modelling skills to simplify the problem to current processing power levels whilst at the same time retaining the most important physical responses. It is the calculation of the cross-sectional stiffness parameters which becomes the main issue in performing accurate analyses of rotor blade designs. The assessment of these properties has been investigated widely with isotropic sections.

The development of a method which can calculate the equivalent 1-D beam properties for arbitrary sections composed of non-homogeneous anisotropic materials is desired by industry. In addition to helicopter rotor blades there are other examples in the aerospace industry where there is a need to accurately model arbitrary shaped tubes. These include propellers and main spars such as those found in the Westland Lynx tailplane. There are modelling opportunities outside of the Aerospace industry too. Sporting equipment such as golf club shafts, tennis rackets and ski poles and offshore platform structures are to name but a selected few examples where closed section composite tubes are subjected to various loads. Potentially, there is scope for optimising the composite lay-up and taper of such structures.

The behaviour of beams is of great importance in the design of engineering structures. The dynamic response of helicopter rotor blades is generally analysed using 1-dimensional beam models with the overall structural properties of the section to reduce processing requirements. The calculation of the beam section properties are therefore critical in achieving accurate 1-dimensional beam properties and a full 6x6 stiffness matrix accounting for the coupling behaviour. There are several methods for calculating the behaviour of arbitrary beams. Most use 2D slice model representations of the section, these include Kosmatka [2], Wörndle [3] and Rand [4]. The most complete of these is Kosmatka's approach which gives a good physical insight into the problem since all displacement functions (including warping) are evaluated. Kosmatka, because of this detail, shows that in-plane warping must be considered in addition to out-of plane warping in the analysis of anisotropic sections.

A generalised method for the analysis of beams with arbitrary cross-sections with non-homogeneous anisotropic material properties is presented. It produces a full 6x6 stiffness matrix

with both material and geometric coupling accounted for. Both in-plane and out-of plane warping are permitted. The approach is finite element based using the MSC PATRAN/NASTRAN software packages, coded using the PCL programming language supplied as part of PATRAN.

The Method - Theory

The method presented here is based on the work of Bartholomew and Mercer [5] which has been extended to produce a full 6x6 stiffness (K) matrix for the beam including material and geometric coupling behaviour. The locations of the elastic centroid, centre of gravity and the shear centre are also calculated. The section properties can then be transformed to act around any of these locations, or any other arbitrary point.

The method analyses a 3-D mesh of a slice through a beam cross-section (see Fig.1). The elements are given material properties in accordance to the cross-section with the correct orientation. The two faces of the slice are linked together using multi-point constraints which allow relative motion between the two based on 6 scalar freedoms – 3 translational and 3 rotational. It is these scalar freedoms which provide the information necessary to produce the 6x6 stiffness matrix and allow in-plane and out-of-plane section warping to occur.

The six equations, which link the nodes on each face of the section and the scalar freedoms, are shown below:

$$u(Q) = u(P) + \mu_1 - \omega_3 y \quad (1)$$

$$v(Q) = v(P) + \mu_2 + \omega_3 x \quad (2)$$

$$w(Q) = w(P) + \mu_3 - \omega_2 x + \omega_1 y \quad (3)$$

$$r_x(Q) = r_x(P) + \omega_1 \quad (4)$$

$$r_y(Q) = r_y(P) + \omega_2 \quad (5)$$

$$r_z(Q) = r_z(P) + \omega_3 \quad (6)$$

where Q are the dependent nodes, P are the independent nodes, x, y are the co-ordinates of the node pair in the section, μ_1, μ_2, μ_3 are the scalar freedoms in translation, $\omega_1, \omega_2, \omega_3$ are the scalar freedoms in rotation, u, v, w are the displacements in translation and r_x, r_y, r_z are the displacements in rotation for the nodes.

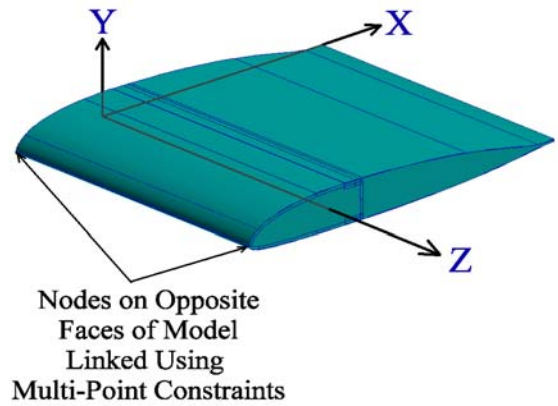


Figure 1: A Beam Section and Associated Structure

The section properties are obtained in two stages. The first stage involves applying unit loads to 4 of the scalar freedoms in turn, i.e. the axial translational, μ_3 , and the three rotational. These represent axial tension, bending about the X-axis, bending about the Y-axis and a torsional moment about the longitudinal X-axis. The scalar freedoms μ_1 and μ_2 have to be restrained to zero to prevent rigid body rotation. This means that the other 4 freedoms can provide flexibility data, but the two shear flexibilities are not available directly from the output. These can be found by integrating the displacements across the entire section and calculating the mean slope [6,7].

The flexibilities for the two shear load cases can be found by using the reaction forces at the nodes caused by the MPCs in the bending load cases (moments applied to the rotational freedoms ω_1 and ω_2 .) These forces are applied to the model at each node with the results for one face reversed. This distributes the shear forces about the section accurately, taking into account the relative stiffness of each element. The magnitudes of all of the forces have to be normalised so that the applied shear force is equivalent to a unit load. This varies with the slice length, so, for example, if the slice model is unity in length, then the forces from the bending case have to be halved to produce a unit load in shear. As before, μ_1 and μ_2 are restrained to zero, so only the other 4 freedoms can provide flexibility data. The shear flexibilities are calculated as before. The complete 6x6 flexibility (S) matrix is now available:

$$\begin{array}{c}
 \text{Second Analysis -} \\
 \text{Shear Calculation}
 \end{array}
 \begin{array}{c}
 \text{First Analysis -} \\
 \text{Shear Calculation}
 \end{array}$$

$$\begin{pmatrix} \delta_x \\ \delta_y \\ \delta_z \\ \theta_x \\ \theta_y \\ \theta_z \end{pmatrix} = \begin{pmatrix} S_{11} & S_{12} & S_{13} & S_{14} & S_{15} & S_{16} \\ S_{21} & S_{22} & S_{23} & S_{24} & S_{25} & S_{26} \\ S_{31} & S_{32} & S_{33} & S_{34} & S_{35} & S_{36} \\ S_{41} & S_{42} & S_{43} & S_{44} & S_{45} & S_{46} \\ S_{51} & S_{52} & S_{53} & S_{54} & S_{55} & S_{56} \\ S_{61} & S_{62} & S_{63} & S_{64} & S_{65} & S_{66} \end{pmatrix} \begin{pmatrix} F_x \\ F_y \\ F_z \\ M_x \\ M_y \\ M_z \end{pmatrix} \quad (7)$$

$$\begin{array}{c}
 \text{Directly From} \\
 \text{Second Analysis}
 \end{array}
 \begin{array}{c}
 \text{Directly From} \\
 \text{First Analysis}
 \end{array}$$

Where δ_x , δ_y , and δ_z are relative displacements of the ends of the beam per unit length, θ_x , θ_y and θ_z are relative rotations of the ends of the beam per unit length, F_x , F_y and F_z are the shear forces and axial force acting in the beam, and M_x , M_y and M_z are the bending moments and torsional moment acting in the section of the beam being considered.

Shear Centre, Elastic Centre

The flexibility matrix produced using this method is based around loading at the origin of the analysis co-ordinate system. However, it should be noted that the flexibilities for the bending and torsion load cases effectively centre around the elastic and shear centres, respectively. This is because an applied moment at the origin is equivalent to a pure moment at the elastic or shear centres, wherever they are located. The method finds the lowest energy solutions for the applied load cases, with the constraint that rotations are based around the axes defined for the beam section prior to analysis. The bending moments are therefore applied around the analysis axes, not the neutral axes of the section.

If the origin does not coincide with the elastic or shear centres, then there will be coupling terms in the axial and shear load flexibilities due to offset loading. The location of the shear centre is governed by the relationship between the amount of torsion due to the applied torsion and shear load cases. The shear load case is centred at the origin, and so applies a torsional moment as well as the shear force. The shear load cases have been normalised to 1N, so the torsional moment is represented by the magnitude of the moment arm. The shear centre is calculated by:

$$X_s = \frac{S_{26}}{S_{66}} \quad (8)$$

$$Y_s = \frac{S_{16}}{S_{66}} \quad (9)$$

where X_s and Y_s are the locations of the shear centre with respect to the origin of the beam. Similarly, the elastic centre is calculated using the relationship of the amount of bending due to the axial and the bending load cases.

$$X_c = \frac{S_{35}}{S_{55}} \quad (10)$$

$$Y_c = \frac{S_{34}}{S_{44}} \quad (11)$$

The flexibility matrix can be transformed to any location desired with standard transformation equations for section properties. The 6x6 stiffness (K) matrix is then produced by inverting the flexibility (S) matrix for the section based at the location to which the properties have been transformed. The matrix contains all coupling behaviour due to material and geometry.

Implementation

The method has been coded as a routine for use with MSC PATRAN [8] in PATRAN Command Language (PCL). The user creates a 2-D mesh of the cross-section of the beam to be analysed, with material properties and orientations defined correctly. The routine takes the mesh, extrudes it into 3-D and reassigns all the material properties and orientations. The MPCs are created, using the locations of the nodes within the cross-section, as described earlier. The first four load cases are then applied and analysed using MSC NASTRAN [9].

Once the analysis is concluded, the routine accesses the results, placing the 4 available flexibilities directly into the flexibility matrix. The shear flexibilities are calculated by integrating the axial displacements of all the nodes in the section to get the mean slope. This is followed by processing the force resultants to produce the shear load cases. The two new shear force load cases are then applied and re-analysed with NASTRAN. The shear flexibilities for the two load cases are calculated in the same manner as before. The flexibility data from the calculations and the scalar freedoms are then added to the now complete flexibility matrix. The matrix can be processed according to the user's requirements, including transformations and inverting to give the stiffness matrix.

Isotropic Rectangular Solid Section

As a check of the method and the analysis code, the first example consists of a simple rectangular section composed of an isotropic aluminium alloy, with the origin of the co-ordinate system at the cross-section centroid. The results should show no coupling behaviour and stiffness properties similar to simple analytical solutions.

The cross-section was 16x10mm and the material data was ($E=70\text{GPa}$ and $\nu=0.3$.) The elements used in this analysis were all 1mm^3 , therefore a total of 160 CHEXA elements were used which had linear displacement functions. 1122 MPCs were required to constrain the slice section model. The results from the stiffness matrix are shown in Table 1. All other results were at least 7 orders of magnitude lower than these six on the leading diagonal, indicating that no coupling behaviour was present.

	Theory	FE	Error
EA (N)	1.120×10^7	1.120×10^7	0.00%
EI_x (N/m ²)	93.33	93.33	0.00%
EI_y (N/m ²)	238.9	238.9	0.00%
GA_{sx} (N)	3.733×10^6	3.701×10^6	-0.87%
GA_{sy} (N)	3.733×10^6	3.765×10^6	0.85%
GJ (N/m ²)	87.91	88.21	0.34%

Table 1: Comparison of Rectangular Cross-Section Properties with Theory

The errors between the method and theory are small, the largest being with the shear stiffness values which were calculated using Stephen's [7] shear coefficient of 0.867. In the FE method, these were calculated using the displacement field of the section which was approximated by the linear element displacement field. It can be seen from the shear stress plot for shear in X (Figure 2) that the stress distribution is close to the parabolic distribution expected, but does not reach zero at the free edges. This is a limitation of the elements being used, not the method itself. The accuracy of the stress field is improved by increasing the number of elements or by using parabolic displacement function elements.

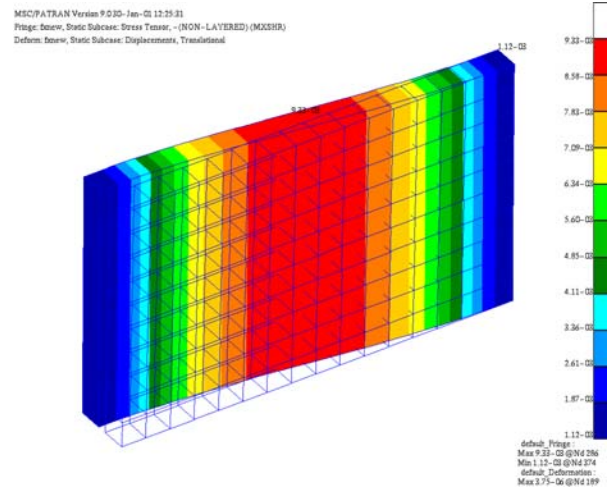


Figure 2: Shear Stress Distribution and Deformed Shape for Rectangular Section

Isotropic Circular Tube

The accuracy of the method when used to predict thin-walled section behaviour was also investigated. The section chosen was a cylindrical isotropic tube with dimensions of an outer diameter of 30mm and a wall thickness of 1mm. A total of 376 linear CHEXA elements were used, the number of MPCs required to link the two faces was 3384.

The stiffness results from the analysis are shown in Table 2. All other values in the matrix were several orders of magnitude lower than these taken from the leading diagonal, reflecting numerical rounding errors, and so were ignored. There is a small difference between the shear stiffness values from this method and the analytical value taken from Stephen. This was due to the relative coarseness of the mesh, and the linear elements inability to produce an accurate deformed shape. The accuracy of this value improved to within 3% when the number of elements through the thickness of the section was doubled. The other properties also showed slight improvements in accuracy. The shear stress distribution for the thin-walled section is shown in Figure 3.

	Theory	FE	Error
EA (N)	6.377×10^6	6.378×10^6	0.01%
EI_x (N/m ²)	671.2	671.3	0.02%
EI_y (N/m ²)	671.2	671.3	0.02%
GA_{sx} (N)	1.304×10^6	1.229×10^6	-5.75%
GA_{sy} (N)	1.304×10^6	1.229×10^6	-5.75%
GJ (N/m ²)	516.3	516.4	0.02%

Table 2: Stiffness Comparison for Hollow Isotropic Circular Section

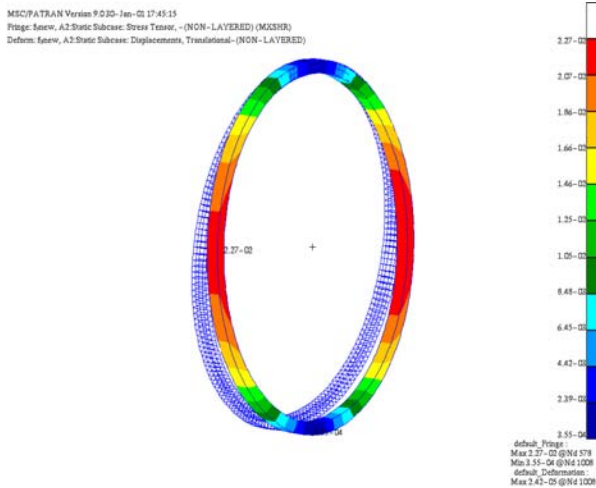


Figure 3: Shear Stress Distribution for Isotropic Hollow Circular Section

Helicopter Rotor Blade

The next example is that of a helicopter rotor blade section, created using approximately 3000 linear elements and 13152 MPCs. Material and geometric information, as supplied by GKN Westland Helicopters Ltd (GWHL) [10], was used in creating the section and finite element mesh. Key material locations were the torque/wing box and a high volume of longitudinal fibres near the nose. The origin of the co-ordinate system was at the nose of the section, with the X-axis passing through the tail of the blade. The material properties excluded anisotropy, so interaction terms were caused only by the geometry (see Eqn 12). The presence of S_{16} and S_{26} terms shows that the shear centre is offset from the tip of the blade (see Fig.4), as would be expected, and is located near the centre of the main torsional wing box. The S_{35} and S_{45} terms show that the elastic centre is also offset from tip of the blade, but not by as much (see Fig.4), its precise location reflecting the action of stiff longitudinal fibres in the nose.

$$\begin{pmatrix} \delta_x \\ \delta_y \\ \delta_z \\ \theta_x \\ \theta_y \\ \theta_z \end{pmatrix} = \begin{pmatrix} 1.68 \times 10^{-8} & -6.55 \times 10^{-8} & 0 & 0 & 0 & 0 \\ -1.53 \times 10^{-8} & 1.12 \times 10^{-7} & 0 & 0 & 0 & 0 \\ 0 & 0 & 5.65 \times 10^{-9} & 1.71 \times 10^{-11} & 2.28 \times 10^{-11} & 0 \\ 0 & 0 & 1.71 \times 10^{-11} & 2.58 \times 10^{-12} & 0 & 0 \\ 0 & 0 & 2.28 \times 10^{-11} & 0 & 2.17 \times 10^{-13} & 0 \\ 2.46 \times 10^{-11} & -2.69 \times 10^{-10} & 0 & 0 & 0 & 2.07 \times 10^{-12} \end{pmatrix} \begin{pmatrix} F_x \\ F_y \\ F_z \\ M_x \\ M_y \\ M_z \end{pmatrix} \quad (12)$$

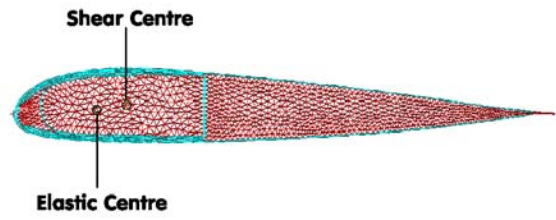


Figure 4: Location of Elastic and Shear Centres for Rotor Blade Example.

An example of the composite in-plane shear stresses due to an applied torsion load is shown in Figure 5. Most of the load is carried by large numbers of $\pm 45^\circ$ plies in the main wing-box area, giving rise to the location of the shear centre. The highest in-plane shear stresses are in a thin layer of $\pm 45^\circ$ plies near the surface above and below the wing-box.

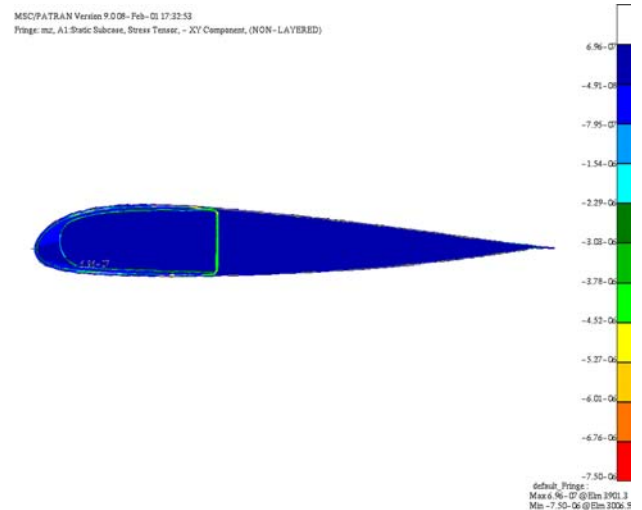


Figure 5: 'In-Plane' Shear Stress Due to Torsional Loading

The flexibilities calculated for the blade compare well with section data from GWHL, giving confidence in both the method and the implementation. Further work using anisotropic sections for aeroelastic tailoring is being carried out. Ideally, comparisons should be made with experimental data, which is intended as part of the development process.

Normal Mode Response of Composite Section

A relatively simple rectangular section (Figure 6) was chosen for linear normal mode analysis. The material properties used are shown in Table 3.

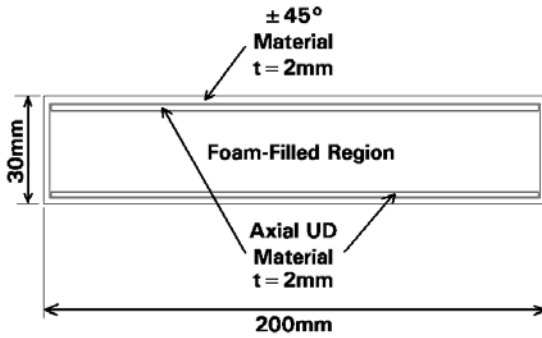


Figure 6: Cross-Section of Normal Mode Example

The example is that of an untwisted blade of length 1000mm. Two finite element models were required for the normal modes analyses, one using shells and solids with the material properties defined in Table 3 and the other made from beams using properties based on analysis of the cross-section (Table 4). The mass properties were calculated by summing all of the density, element cross-section area and centroid location terms in accordance with standard theory [11].

Property	Carbon/Epoxy Composite	Generic Foam
E_1 (GPa)	131.5	0.07
E_2 (GPa)	9.2	0.07
E_3 (GPa)	9.2	0.07
ν_{12}	0.3	0.4
ν_{13}	0.3	0.4
ν_{23}	0.45	0.4
G_{12} (GPa)	4.88	0.025
G_{13} (GPa)	4.88	0.025
G_{23} (GPa)	3.10	0.025
Density (kg/m^3)	1600	51

Table 3: Material Properties for Normal Mode Models

Structural Property	Value	Mass Property	Value
EA (N)	1.203×10^8	Area (m^2)	.006
EI_{11} (Nm^2)	1.787×10^4	Mass/unit length (kg/m)	2.921
EI_{22} (Nm^2)	3.988×10^5	Mass Moment (ρI_{11}) (kgm^4)	0.00045
GJ (Nm^2)	2.018×10^4	Mass Moment (ρI_{22}) (kgm^4)	0.011
$k_1 GA$ (N)	2.611×10^7	Torsional Mass Moment (ρJ) (kgm^4)	0.011
$k_2 GA$ (N)	1.172×10^6		

Table 4: Section Properties for Beam Elements

When modelling a prismatic composite structure using a 1-D general beam section with an

isotropic material, it is not usually possible to get all of the mass and stiffness terms correct. This is due to the difference in I_{11} and I_{22} requirements between the mass and stiffness terms. Therefore, some properties are only approximate to the values calculated by the method. The key products to calculate exactly for the beam model to give good natural frequency results are the torsional mass moment of inertia (ρJ), the torsional stiffness (GJ), the mass per unit length and EA, EI_{11} & EI_{22} . These values alone should give rise to good correlation between shell and beam models of the natural modes of the structure. This is because the critical mass and stiffness terms of the models are virtually identical.

The properties used in the beam model analysis are shown in Table 5. In terms of the overall mass and structural properties of the beams, it is only the bending mass moments of inertia which are inaccurate (4% and 9% too high for ρI_{11} and ρI_{22} , respectively.) This is not an important issue because the mass moments of inertia are insignificant compared to the mass of the slender beam being accelerated by the 'flap' and 'lag' modes.

Section Property	Value	Material Property	Value
A (m^2)	.006	E (N/m^2)	2.01×10^{10}
I_{11} (m^4)	8.93×10^{-7}	G (N/m^2)	8.88×10^8
I_{22} (m^4)	1.99×10^{-5}	ρ (kg/m^3)	486.67
J (m^4)	2.27×10^{-5}		
k_1	4.90		
k_2	0.22		

Table 5: Section and Material Properties Assigned to Beam Model Elements

The normal mode results for the shell and beam models are shown in Figure 7. The model has stress-stiffening based on a centrifugal loading due to a spin speed of 15Hz (900rpm). As a check, the reaction forces at the hub for both models were 12.97kN, matching $F = m r \omega^2$.

The frequencies compare well with each other for each of the three modes. The beam model tends to be stiffer, which is due to the beam formulation not accounting for cross-section deformation which occurs in the shell and solid model.

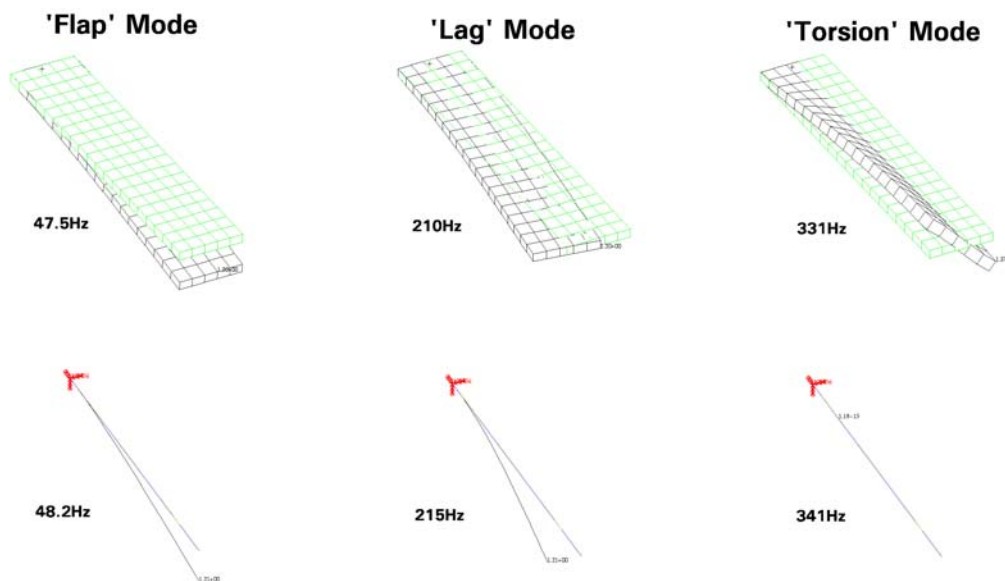


Figure 7: Comparison of Natural Modes for Non-Twisted Shell and Beam Models

Conclusions

A method for calculating the stiffness properties of non-homogeneous anisotropic beams with arbitrary shapes has been presented. It provides a full 6x6 stiffness matrix, giving coupling terms due to geometric and material related effects. It has been shown to give results that compare favourably with elementary theory for a number of simple cases involving isotropic materials, including solid and thin-walled sections. An analysis of a helicopter rotor blade composed of 14 different materials produced results that predict the elastic and shear centres as well as the flexibility matrix. The normal mode response of a composite beam with equivalent properties compared well with a shell model of the same construction.

The use of standard finite element analysis software also allows the user to investigate the stress fields for all the load cases. A useful feature of this is the availability of the interlaminar stresses, allowing delamination prediction to be carried out, if desired.

Acknowledgements

The authors thank GKN/Westland Helicopters for their continued support, especially Pete Wood and Dave Swabey for discussions and information. The EPSRC is also thanked for financial support under contract number AERO RB0861.

References

1. Mansfield, E.H. and Sobey A.J. :*The Fibre Composite Helicopter Blade*, Aeronautical Quarterly, pp.413-417, May 1979.
2. Kosmatka, J.B., Dong, S.B. *Saint-Venant Solutions for Prismatic Anisotropic Beams*. International Journal of Solids and Structures, Vol.28, pp.917-938, 1982.
3. Wörndle, R. *Calculation of the Cross-Section Properties and the Shear Stresses of Composite Rotor Blades*. Vertica, Vol.6, pp.111-129, 1982.
4. Rand, O.J. *Fundamental Closed-Form Solutions for Solid and Thin-walled Composite Beams Including a Complete Out-of-Plane Warping Model*. International Journal of Solids and Structures, Vol.35, pp.2775-2793, 1997.
5. Bartholomew, P., Mercer, A.D. *Analysis of an Anisotropic Beam with Arbitrary Cross-Section*. Royal Aircraft Establishment, Farnborough, Technical Report 84058, 1984.
6. Cowper, G.R. *On the Accuracy of Timoshenko's Beam Theory*, Journal of the Engineering Mechanics Division, Proceedings of the ASCE, Vol.94, No.EM6, pp.1447-53, 1968.
7. Stephen, N.G. "Timoshenko's Shear Coefficient From a Beam Subjected to Gravity Loading", Journal of Applied Mechanics, Vol.47, pp.121-127, 1980.
8. MSC PATRAN Version 9.0, MacNeal-Schwendler Corporation, 2975 Redhill Avenue, Costa Mesa, California 92626, USA.

9. MSC NASTRAN Version 70.7, MacNeal-Schwendler Corporation, 2975 Redhill Avenue, Costa Mesa, California 92626, USA.
10. Private communication , GKN Westland Helicopters, Yeovil, UK 2000.
11. Young, W.C. "Roark's Formulas for Stress and Strain", 6th Edition, McGraw Hill Book Company, 1989.